Cite this article
Vonsul M-I, Knight A, Sabzi M *et al.*
Cottonseed oil–derived resin system for use in bio-based artificial leather.
Green Materials,
https://doi.org/10.1680/jgrma.26.00040

Research Article
Paper 2600040
Received 03/03/2026; Accepted 03/03/2026

Green Materials

Cottonseed oil–derived resin system for use in bio-based artificial leather

Marta-Ievheniia Vonsul
Department of Coatings and Polymeric Materials, North Dakota State University, Fargo, USA

Austin Knight
Department of Mechanical Engineering, North Dakota State University, Fargo, USA

Mohammad Sabzi
Department of Mechanical Engineering, North Dakota State University, Fargo, USA

Renuka Dhandapani
Cotton Incorporated, Cary, USA

Long Jiang
Department of Mechanical Engineering, North Dakota State University, Fargo, USA

Dean C. Webster
Department of Coatings and Polymeric Materials, North Dakota State University, Fargo, USA (Orcid:0000-0002-5765-9514) (corresponding author: dean.webster@ndsu.edu)

In this study, a method of using cottonseed oil as the main component for the preparation of bio-based compositions for the new generation of artificial leather was investigated. Genuine leather is considered a renewable, bio-based product. However, ecological issues caused by leather processing have led to a significant productivity decrease in this industry. As a result, artificial leather, made of polyvinyl chloride and polyurethane, has been commonly used in both industrial and commodity applications. These synthetic alternatives show similar properties to genuine leather but are composed of fossil oil–based materials. Therefore, extensive research is being conducted to utilize renewable materials in the manufacturing of artificial leather. The cottonseed oil–based leather prototype was prepared according to the classic three-layer structure approach that is currently used in synthetic leather manufacturing. Epoxidized cottonseed oil was used to create the top and foamed layers of leather, while the third layer consists of cotton fabric. The properties of the individual layers of leather were evaluated using thermogravimetric analysis, differential scanning calorimetry, dynamic mechanical analysis, and scanning electron microscopy. By combining all layers, artificial leather prototypes were fabricated. Layers made of functionalized cottonseed oil possess flexibility and softness characteristic of traditional synthetic leather.

Keywords: artificial leather/cottonseed oil/green polymers/plant oils/renewable resources/sustainable materials/UN SDG 12: Responsible consumption and production

1. Introduction

Society has recognized the importance of implementing sustainable strategies across all sectors of modern life, and the leather industry is no exception. Although genuine leather is a renewable, bio-based product, its manufacturing process has raised many ecological concerns.[1–6] Simultaneously, the number of people opposing products of animal origin is growing.[7–9] All these factors pose new challenges in developing products from genuine leather. Companies that make genuine leather for consumer products have been under pressure to develop cleaner technologies. Therefore, since the 1950s, artificial leather made of polymeric systems has been commonly used in various applications.[10,11]

The most widely used polymeric materials for the production of artificial leather are polyvinyl chloride (PVC) and polyurethane (PU).[12–16] To imitate animal-based leather, artificial leather is made of a multilayer structure that consists of a base coating layer, a foamed layer, and a fabric layer (Figure 1). The production process of artificial leather can be divided into four main steps. In the first step, a polymer formulation (base layer) is applied onto a substrate (e.g. release paper) that can be easily removed after the process is completed.[19] The formulation typically consists of 55% polymer (PU/PVC), 40% plasticizer, and 5% additives. By pressing the formulation between heated rollers, a thin base layer is formed. In the second step, a foaming formulation comprising a blowing agent is applied on top of the base layer. Curing the formulation in the oven provides the formation of a thick foamed layer. The third step involves the attachment of fabric to the foamed layer and release of the substrate from the bottom of the base layer. The last step of manufacturing is optional and can be realized by passing the layered structure through rollers that provide texture and a leather-like appearance.[17]

Artificial leather made from PU and PVC exhibits competitive properties compared with genuine leather in terms of both mechanical properties and functionality.[20,21] However, a growing

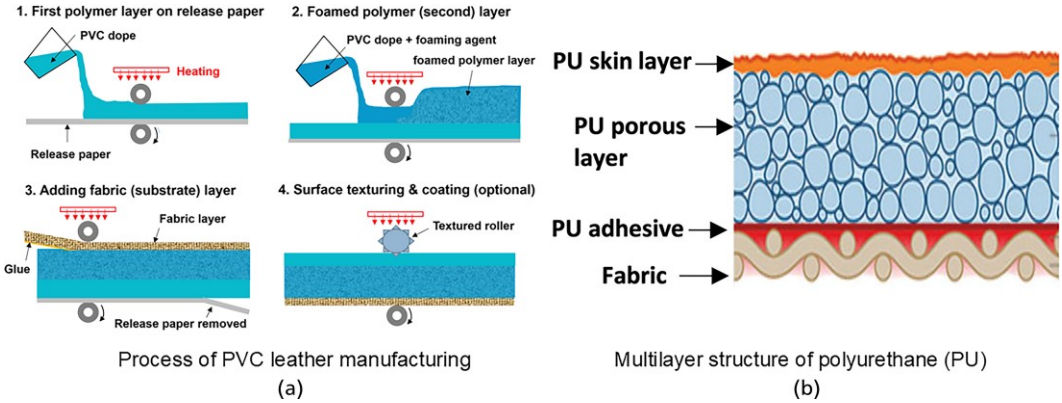

Figure 1. The manufacturing process and multilayer structure of PVC or PU artificial leather. Figure 1(a) is adapted from reference [17] with permission from Elsevier and Figure 1(b) is adapted from reference [18] with permission from Covestro LLC.

number of people have realized that it is not a sustainable product since it is composed of petroleum-derived polymers.[22,23] To address this problem, different renewable resources have been proposed as alternatives to replace or partially substitute fossil-based polymers in leather manufacturing.[24–26] For example, C. Alvarez A. Hijosa reported the use of fibers from pineapple leaves, which are considered waste after pineapple harvesting in leather development.[27] A combination of pineapple leaf fibers and polylactic acid fibers were used to form a nonwoven material that serves as the main layer of leather. A top PU coating, which accounts for 10%–15% of the total material weight, is applied to increase the performance of the leather.

Another example of an eco-friendly leather from renewable sources is a coated textile made from grape pomace. The production process includes drying grape pomace and mixing it with PU to make a thin, nonfoam layer and a foamed layer. A type of vegan leather, which is known as 'grape leather' or 'wine leather', is obtained by applying these layers over a cellulosic textile carrier.[28,29]

Fungal leather has also been featured as an environmentally friendly leather-like substitute material.[30–32] Fungi grow naturally by generating microscopically interconnected tubular cells that eventually form mycelium. Fungal mycelium is a solid, foam-like material, which consists of fibrous networks that imitate the structure of an animal skin. This material can be treated by different physical and chemical methods to have leather-like textures, colors, and strength.[3,23] Several other materials, such as cactus fiber, apple residues, teak leaves, silk proteins, and so on, have also been previously offered as raw materials for bio-based artificial leather.[22,28,33,34]

Despite the broad commercial interest, the new generation of currently proposed bio-based leathers are fabricated from unconventional biomaterials, which makes these products very expensive. Furthermore, the majority of the alternative leathers contain PU layers that play a vital role in their performance.[35] Leather technologies that use readily accessible renewable materials as feedstocks have not been developed and are in great demand. In addition, it is worth noting that the commercial potential of such technologies highly depends on their manufacturing technologies. The most promising ones are those that can be implemented using existing leather production equipment and processes without significant modifications.

Our ultimate goal is to develop artificial leather using widely available biomaterials. Given their abundance and renewability, oils from agricultural sources have been intensively investigated in different areas as potential replacements for petroleum-based polymers.[36–38] Various chemical modifications of triglycerides, with epoxidation being the most important, produce oligomer resins that can be further converted into useful thermoset polymers.[39–43] A common drawback of plant oil–based thermosets is their low glass transition temperature, which is attributed to their long flexible chains and results in low modulus and high flexibility. Currently, the primary application of epoxidized vegetable oils is as plasticizers.[44–48] In this work, the authors show that the flexibility of plant oil–derived thermosets offers an advantage in artificial leather. The authors explore plant oils to fabricate the layers of artificial leather using cottonseed oil as an example. All layers of artificial leather were produced from cotton-derived materials. The leather was prepared using the classic three-layer structure approach, where the top layer and the middle layer were made from polymeric resin and the bottom (substrate) layer from cotton fabric. Epoxidized cottonseed oil (ECO) was used as the major ingredient in fabricating the base and the foamed layers of leather. To the best of the authors' knowledge, this is the first report of an artificial leather composition developed from plant oil–derived materials.

2. Experimental section

2.1 Materials

ECO was synthesized using a method reported earlier.[49] The epoxy equivalent weight of the resin was determined via hydrogen bromide titration (ASTM D1652) and the value was 264.8 g/eq. Dodecenyl succinic anhydride was purchased from VWR (Radnor, PA). BV-CAT 7 catalyst was provided by Broadview Chemicals (Newark, New Jersey). Azodicarbonamide (ADA) foaming agent and zinc oxide (accelerator, decomposition catalyst) were received from Sigma Aldrich (St. Louis, MO). Tegostab B 8993 surfactant (polyether-polydimethylsiloxane copolymer) was kindly provided by Evonik (Piscataway, New Jersey). All materials were used as received without further purification.

2.2 Preparation of leather top layer

ECO and dodecenyl succinic anhydride curing agent were used for the preparation of the top layer. The ratio of epoxy to anhydride (ECO: anhydride) was fixed at 1:1.5, based on equivalent weights. BV-CAT 7 catalyst was added to the epoxy-anhydride formulations to ensure efficient polymerization. The amount of catalyst was fixed at 3% by the total weight of the epoxidized oil and the anhydride. The preparation of the top layer is as follows. ECO, anhydride, and catalyst were mixed at 3500 rpm for 3 min in a FlackTek high-speed mixer. Following this, the formulations were transferred into glass vials and precured on a hot plate while continuously stirring at 120°C. After precuring, the formulations were applied using a drawdown bar at 25 mil on cleaned glass panels and steel panels (Q-Lab, QD-36). The panels were put in a preheated oven and cured at 160°C for 30 min.

2.3 Preparation of leather foamed layer

The foamed layer was prepared using a procedure similar to the base layer. ADA blowing agent and zinc oxide were used in the formulations to enable foaming. The amount of ADA in the formulations was fixed at 3 pph (pph = parts per hundred of the total weight of epoxidized oil and anhydride), while the amount of ZnO was kept at 0.5 pph. ADA and ZnO were added to the previously prepared mixture comprising ECO, anhydride and catalyst. Surfactant was used to ensure the formation of a homogeneous cell structure. The amount of surfactant was kept at 0.5 wt.%. The formulations were mixed in a Flacktek Speed high-speed mixer at 3500 rpm for 3 min. The formulations were precured at 120°C on a hot plate. After precuring, formulations were poured into silicone molds with different shapes or applied on glass panels using a drawdown bar at 15 mil. Specimens were cured at 160°C for 30 min.

2.4 Preparation of leather prototype

The leather prototype was prepared by a three-layer structure method. In this method, the foamed formulation was layered on top of the fabric layer, followed by applying the top layer over the foamed layer. All three layers, the base layer, the foamed layer, and the fabric layer, were based on cotton derivatives. Detailed description of the preparation procedure is given in the last section of this manuscript.

2.5 Characterization methods

The physical properties of the top layer, applied on metal panels, were evaluated according to ASTM International coating standards. The hardness was determined by subjecting coatings to König pendulum hardness (ASTM D4366) and pencil hardness (ASTM D3363) tests. In the König pendulum hardness test, the time taken for the oscillating pendulum to decrease its amplitude from the 6° deflection angle to 3° is measured. The more flexible a coating is, the faster the amplitude decreases. The results were reported in seconds. In the pencil hardness test, pencils with hardness values from 8H (the hardest) to 9B (the softest) were pushed across the sample. The hardest pencil that could not produce a visible scratch on the coating was reported. Adhesion to the substrates was characterized by a cross-hatch adhesion test (ASTM D3359). Loss of adhesion was reported according to the scale from 0B to 5B, where 0B indicates full delamination of coating from the metal surface. Conical mandrel bend (ASTM D522) was performed to determine flexibility of the coatings, namely, resistant to cracking upon bending. Reverse impact strength (ASTM D2794) was conducted to define resistance of material to rapid deformation using a Gardner Impact Tester. The drop weight was 4 lb and the maximum drop height was 43 in. The results were reported in inch-pounds. Chemical resistance of the coatings films was determined using the methyl ethyl ketone (MEK) double rubs test (ASTM D5402). A cheesecloth was wrapped around a hammerhead and soaked in MEK. The results were reported as the number of double-rubs a coating can withstand until coating damage was observed. Dry film thickness was measured with a Byko-Test 8500 thickness gauge.

Gel content of the top layer films was determined via Soxhlet method. Samples were placed in a paper thimble, which was then inserted into a Soxhlet extractor. Toluene was refluxed through the extractor for 24 h. Samples were removed from the thimble and dried in the oven for several hours. The weight of the samples was measured, and the gel content was calculated as the final weight/initial weight. The results were reported as a percentage.

Differential scanning calorimetry (DSC) was performed using a TA Instruments Discovery DSC 2500 differential scanning calorimeter. Nitrogen was used as a purge gas. Depending on the samples, hermetic aluminum pans (liquid formulation) or standard aluminum pans (cured films) were used. The weight of the samples was 5–10 mg. Experiments were run at a heating rate of 5°C/min from 25°C to 250°C. In the case of the cured films, the scans were performed in a heat-cool-heat mode (temperature range −50°C-250°C).

Thermogravimetric analysis (TGA) was run on a TA Instruments Discovery TGA 550 thermogravimetric analyzer. Samples were placed in tared platinum pans and heated from room temperature

to 600°C with a heating rate of 10°C/min in a nitrogen atmosphere. The weight of the samples was 5–12 mg.

Viscosity measurements were performed using a Brookfield CAP 2000 cone/plate viscometer. To analyze the viscosity, samples were placed between the cone and the plate of the viscometer and subjected to shear. Measurements were taken four times for each sample at temperature 24 ± 0.4°C using cone spindle CAP 03 (shear rate = 133 s^{-1}) at 100 rpm. The measured average viscosity was reported.

Dynamic mechanical analysis (DMA) was conducted on a TA Instruments Discovery DMA 850 dynamic mechanical analyzer using a single cantilever geometry. The temperature was raised from −50°C to 200°C with a heating rate of 5°C/min. The glass transition temperatures (T_g) of the samples were defined as the tan δ peak. The storage moduli (E') were determined at 60°C above the T_g. The cross-link densities (v_e) of the thermosets were calculated by following equation:

$$E' = 3v_eRT.$$

where $E'$is the storage modulus in the rubbery plateau region, R is the gas constant and T is the absolute temperature.[50]

Optical microscopy was used to analyze the foamed samples. Microscopic images were taken on a Keyence VNX-7000 Digital Microscope.

Scanning electron microscopy (SEM) was used to study the morphology of the foamed samples. A slice (∼5 mm thick) of each foam sample was cut by hand with a double-edged razor blade. Slices were attached to cylindrical aluminum mounts with silver paint (SPI Products, West Chester, Pennsylvania) to view the cross section, and then sputter coated (Cressington 108auto, Ted Pella, Redding, California) with a thin layer of gold. Images were obtained with a JEOL JSM-6490LV scanning electron microscope (JEOL USA, Inc., Peabody, Massachusetts) at an accelerating voltage of 15 kV.

Micro-computed tomography (micro-CT) was used for imaging the internal structure of the ECO-based foams and to define their porosity. Foamed samples were scanned in a GE Phoenix v|tome| x s X-ray CT system equipped with a 180-kV nanofocus X-ray tube and a high-contrast GE DXR250RT flat panel detector (GE Sensing & Inspection Technologies GmbH, Niels Bohr Str 7, 31515 Wunstorf, Germany). At a voltage of 80 kV and a current of 500 µA with a diamond target, 1500 projections were acquired. Detector timing was 100 msec. Sample magnification was 12.27× with a voxel size of 16.3 µm. Acquired images were reconstructed into a volume data set using GE datos|x 3D computer tomography software version 2.2 (GE Sensing & Inspection Technologies GmbH, Niels Bohr Str 7, 31515 Wunstorf, Germany). The reconstructed volume was then viewed and porosity analysis was performed using VGStudio Max version 2023.3 (Volume Graphics, Inc., 3219 Arbor Pointe Drive, Charlotte, North Carolina).

3. Results and discussion

Currently, synthetic leather is manufactured on a mass scale using well-established processes. Integrating new bio-based materials with established manufacturing technology represents the most promising approach to developing innovative bio-based leather. In view of this, in this study we produced leather samples with a three-layer structure (Figure 2) similar to commercial synthetic leather using ECO as the resin.

In this approach, the leather is prepared by a typical manufacturing method, where the top layer and the foamed layer are made from ECO thermoset resin and the third layer from fabric. Each layer serves its specific function. The top layer is needed for the protection of the internal foamed layer and for the creation of the 'natural' grain and texture of real leather. In addition, by using colorants, the top layer can be produced in various colors. The porous structure of the foamed layer provides the soft, warm feel typical of genuine leather. The fabric layer, which is composed of woven or nonwoven textiles, gives the leather most of its strength. Overall, all layers should be made from materials that can replicate the pliable quality of genuine leather. This study demonstrates the fabrication of leather prototypes from cottonseed oil. However, other types of vegetable/plant oils could also be utilized. The use of cottonseed oil in the composition has some advantages. The main benefit is the more flexible nature of cottonseed oil–based resins compared with resins made from oils with a higher degree of unsaturation.[49]

3.1 Preparation and properties of the top layer

The top layer is produced first in the industrial manufacturing process of synthetic leather. In this study, this layer was prepared by reacting ECO with dodecenyl succinic anhydride (DDSA). In our previous work, we examined the curing conditions of ECO with DDSA to produce bio-based foams.[51] It was determined that the optimal ratio of epoxy to anhydride was 1:1.5 (based on equivalent weight), and the best curing conditions were 160°C for 30 min. We applied the same process in this study to assess whether the ECO-based thermoset can serve as the top layer of the leather composition. BV-CAT 7 catalyst was added to the formulation to

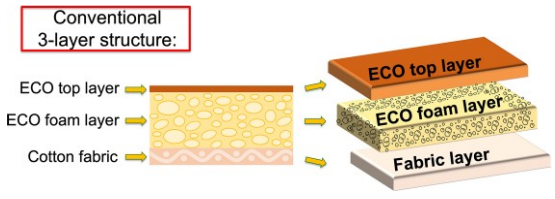

Figure 2. Structure of ECO-based artificial leather

accelerate the reaction rate between ECO and anhydride and to link the anhydride in the early stage of the reaction. A considerable amount of anhydride could be lost due to evaporation if no catalyst is used, as discussed below.

The formulations were applied to metal panels and cured for 30 min at 160°C. The resulting films were tack-free after curing, and their properties were examined according to ASTM standards. The films exhibited modest chemical resistance, demonstrating only 50 double rubs in the MEK double rub test (ASTM D5402). The nonisothermal DSC thermogram of the cured films revealed no exothermic peaks, indicating complete curing. Soxhlet extraction on the sample produced an average gel content of 91.3%. To investigate the cause of the sample's low chemical resistance, the same formulation was cured at lower temperatures for longer durations: 120°C for 2 h and 150°C for 5 h. The gel content of the new samples was 96.9%, which was only slightly higher than that of the sample cured at 160°C for 30 min despite the significantly longer curing time. Furthermore, the MEK test results still showed low chemical resistance of the new samples.

To investigate the issue further, TGA experiments of the formulation and DDSA were conducted. In Figure 3, the formulation shows a mass loss starting at 150°C, corresponding to the mass loss of DDSA at the same temperature range, which suggests that the mass loss of the formulation can be attributed to the evaporation of DDSA. The epoxy resin does not contribute to this weight loss because its degradation starts at 298°C. These results explain the low solvent resistance of the ECO-based films. During the curing process at 160°C, a certain amount of DDSA most probably evaporated and led to a low cross-link density of the cured films. The higher gel content achieved at 120°C/2 h and 150°C/5 h is attributed to reduced DDSA loss and extended curing time. However, the poor chemical resistance of the sample cured even at 120°C indicates that the loss of the curing agent still takes place at this temperature. To overcome this challenge, a precuring stage,

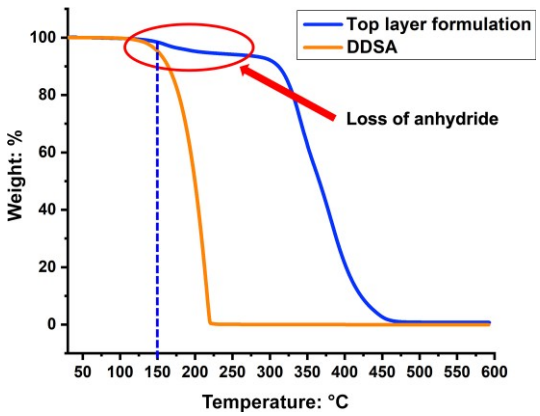

Figure 3. Thermogravimetric curves of uncured top layer formulation and DDSA

during which the formulation was heated to the start temperature of the reaction in a closed system to allow partial reaction, was incorporated into the curing procedure.

A DSC scan of the formulation was used to determine the precuring temperature. Figure 4(a) shows the thermogram of the formulation. The exothermic peak indicates the cross-linking reaction, which starts at about 120°C and peaks at around 160°C. Therefore, 120°C was chosen as the precuring temperature.

The precuring was performed in reaction vials for three different durations: 60, 90, and 120 min. As expected, the viscosity of the formulation increased after curing, from 0.54 Pa·s before curing to 5.78 Pa·s after 1 h of precuring (both viscosities measured at 24°C and 100 rpm). The increase in viscosity is due to the increase in molecular weight as a result of the epoxy-anhydride reactions. To analyze the formulation's curing behavior further, DSC was conducted on the precured formulations to monitor the progress of the epoxy-anhydride reaction after the precuring stage. As shown in Figure 4(b), all the samples display exothermic peaks around 160°C, indicating the cross-linking reaction of the uncured part of the formulation. This is expected because the precuring is intended to partially react the resin components to prevent significant volatilization of the cross-linker.

The total enthalpy of the reactions (ΔH) for the three samples shown in Figure 4(b) can be determined by calculating the areas under their corresponding exothermic peaks. ΔHs for the three samples and uncured formulation are summarized in Table 1. ΔH decreases with longer precuring times because less uncured resin remains after precuring. This difference indicates the progress of the reaction between ECO and DDSA during the precuring stage.

The curing behavior of the formulation was also investigated in a two-stage curing cycle. In the first stage, the formulations were precured at 120°C for 60, 90, and 120 min. The precured formulations were then applied to metal panels and cured in an oven at 160°C for 30 min. The cured samples were studied using DSC, and the results are shown in Figure 4(c). No exothermic peaks are detected on the thermograms of any of the samples, indicating the completion of the reaction between ECO and DDSA after the two-stage curing process. The chemical resistance of the samples was evaluated using the MEK double rub test and all demonstrated good chemical resistance with more than 200 MEK double rubs. Based on these findings, it is suggested that a precuring stage be included in the manufacturing of ECO-based thermosets, especially when the end products require good chemical resistance. The optimal condition for precuring is 120°C for 60 min.

Other properties of the two-stage cured sample, such as hardness and adhesion strength, were also tested to better understand its performance. The König and pencil hardness test results indicate low hardness of the sample (Table 2). It also exhibits the highest possible value in the reverse impact resistance test and passes the

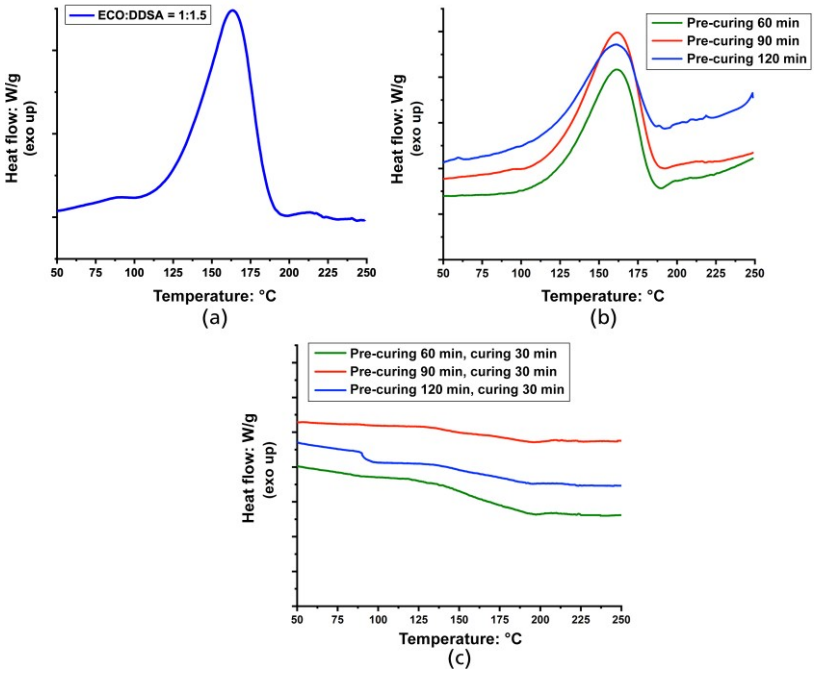

Figure 4. (a) Nonisothermal DSC thermogram of the top layer formulation; (b) nonisothermal DSC curves of the top layer formulation after being precured at 120°C for different durations; and (c) nonisothermal DSC scans of the films cured by a two-stage curing process

Table 1. Reaction enthalpies determined from DSC analysis

Formulation	ΔH: J/g
Uncured	104
Precured for 60 min	68
Precured for 90 min	59
Precured for 120 min	47

Table 2. Properties of the top layer prepared by the two-stage curing process: precuring at 120°C for 1 h followed by final curing at 160°C for 30 min

Properties	ECO:DDSA ratio 1:1.5; 3% BV-Cat 7
König hardness (s)	12
Thickness (μm)	220 ± 3.85
Cross-hatch adhesion	5B
Pencil hardness	7B
Reverse impact (in•lb)	>168.56
Conical mandrel bend	PASS
MEK DR	200

conical mandrel bend test, demonstrating extremely high flexibility. The flexible properties of the sample are demonstrated in Figure 5 and Video 1 (Supplementary Information).

The demonstrated properties are directly attributed to the flexible nature of the ECO-based resin. The fatty aliphatic chains present in the ECO significantly influence the material's flexibility. In addition, the aliphatic molecular structure of the anhydride cross-linker also contributes to the properties of the sample. The combination of these two reactants through cross-linking results in a network that provides the material with good mechanical robustness and flexibility. Furthermore, the sample exhibits strong adhesion to steel substrates, as indicated by the results of the cross-hatch adhesion test. While this property is not crucial for leather applications, it may be advantageous in other potential uses. It is worth noting that the properties listed in Table 2 are measured from samples prepared according to a curing schedule of 120°C for 1 h (precuring) and 160°C for 30 min (second-stage curing). However, films prepared with longer precuring times show very similar properties.

The thermomechanical properties of the top layer were also evaluated using TGA and DMA, and the results are presented in Figure 6 and Table 3. The TGA results show that the initial decomposition temperature, which corresponds to a 5% mass loss of the material, is around 310°C, indicating its high thermal stability. The material almost fully decomposes around 445°C. The glass transition temperature T_g, determined from the tan delta (δ) peak of the DMA test, is 22°C, and the sharp peak indicates a uniform and homogeneous network structure of the sample. Despite the relatively low value of the cross-link density, the material exhibits good thermal and solvent resistance. Based on these results, it is expected the sample is suitable for its potential use as the top layer of bio-based leather.

Figure 5. Demonstration of the flexibility of the top layer sample

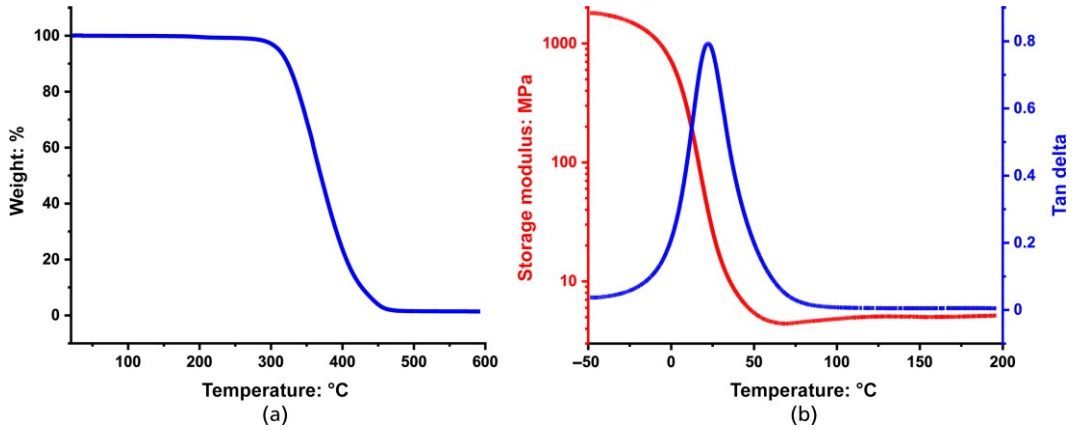

Figure 6. (a) TGA and (b) DMA curves of the top layer

Table 3. Thermomechanical properties of the top layer

Properties	ECO:DDSA ratio 1:1.5; 3% BV-Cat 7
Initial decomposition temperature, $T_{d\ (5\%)}$: °C	310.87
Temperature of 50% weight loss, $T_{d\ (50\%)}$: °C	369.62
Temperature of 95% weight loss, $T_{d\ (95\%)}$: °C	445.11
Glass transition temperature, T_g: °C	22.19
Storage modulus E´ (at T_g + 60°C): MPa	4.599
Cross-link density, v_e: 10^3 mol/m^3	1.36

3.2 Preparation and properties of the foamed layer

The foamed layer was created by foaming the same formulation that was used to produce the top layer. Two methods were used to produce the foam, and in both methods, the foaming agent (ADA) and accelerator (zinc oxide) were fixed at 3 pph and 0.5 pph, respectively. In Method 1, ECO, DDSA, BV-CAT 7, ADA, and zinc oxide were mixed in a Flacktek high-speed mixer for 3 min and precured at 120°C for 1 h. The precured formulations were poured into silicone molds and cured in the oven at 160°C for 30 min. In Method 2, ECO, DDSA, and BV-CAT 7 were mixed in the high-speed mixer for 2 min and precured at 120°C for 1 h. After that, ADA and zinc oxide were added into the precured formulation, and the mixture was mixed again for 3 min before being poured into molds and cured in the oven at 160°C for 30 min.

Both methods resulted in successful curing and foaming of the formulations. Samples from the two methods demonstrated a similar degree of expansion but different cell morphology. The foam prepared by Method 1 displays a higher cell density (number of cells/unit area) than the foam prepared by Method 2, as shown in Figures 7(a) and 7(b). As a result, the first foam exhibits a lower density and is softer (easier to compress). In addition, the foam made using Method 2 appears to contain undecomposed ADA, while the sample by Method 1 is free of it, as illustrated in Figures 7(c) and 7(d). The presence of ADA residues in the Method 2 sample can be attributed to the imbalance between the curing and foaming processes, which will be discussed later.

SEM was utilized to further study the morphology of the foams. Both foams contain a mixture of open and closed cells; however, most of the cells of the foam prepared by Method 2 are closed ones (Figures 8(a) and 8(b)). The broad cell size distribution in both cases can be attributed to the absence of a surfactant in the formulation, which can stabilize the growing cells. A surfactant was not used in this study because of our focus on determining the effects of the two preparation methods. SEM images also confirm the higher cell density of the foam prepared by Method 1 as observed from the optical images. Micro-CT was additionally employed to quantify the porous structure of the foams. Figures 8(c) and 8(d) shows cross sections of the two foams, with the Method 1 foam displaying a denser cell distribution, which

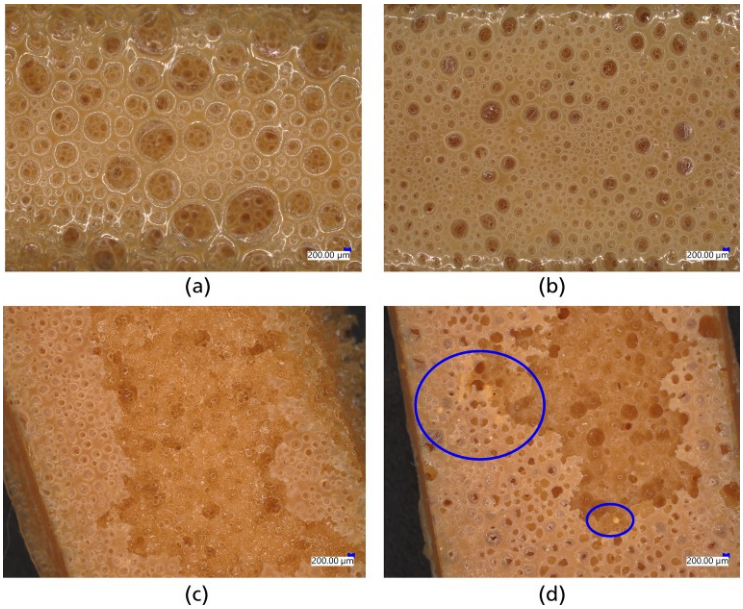

Figure 7. Optical microscopic images of foamed samples prepared by Method 1 (a) and (c) and by Method 2 (b) and (d). Top surfaces shown in (a) and (b), bottom surfaces in (c) and (d)

aligns with the results from the optical and SEM studies. The porosity of the foams was calculated using the equipment's analysis software, and the results show that Method 1 foam exhibits a significantly higher porosity than the Method 2 one (Table 4). The differences in the morphology and porosity of the two foams can be attributed to their different foaming kinetics. Curing and foaming occur simultaneously, competing with each other during the foam manufacturing process. Foams with different morphologies can be produced depending on which process is more dominant, as discussed below.

The process of foam fabrication involves curing the resin and foaming the material in one single operation.[52] The overall reaction kinetics depends on the curing kinetics of the epoxy-anhydride network and the decomposition kinetics of the blowing agent.[53] The two processes must occur at a suitable rate ratio to produce a homogeneous cell structure. Depending on which process is dominant, foams with different morphologies can be produced. Figure 9 demonstrates the main effects of curing and foaming on properties of the polymer foams. Curing leads to a gradual increase in the viscosity of the formulation, which significantly affects the nucleation, growth, and coalescence of the cells. If foaming occurs too quickly, the viscosity of the formulation may still be low when the cells begin to grow, leading to larger cells, cell coalescence (creating interconnected open cells), or even catastrophic cell rupture and gas escape from the material. In this study, both foaming methods showed no signs of significant cell rupture or gas escape. In Method 1, curing and foaming occurred concurrently, meaning that cells started to expand when the viscosity was relatively low. In Method 2, cells grew in a higher-viscosity environment due to the precuring process. As a result, the foam prepared by the latter has a lower porosity and more closed cells. In addition, in the second method, the foaming agent and accelerator were incorporated into a precured formulation, whose relatively high viscosity could cause inhomogeneous dispersion of the particles. Due to the agglomeration, the interaction between the foaming agent and the accelerator was hindered, which led to a suppressed decomposition (gas-generating) rate.[54] This also contributed to the lower porosity of the foam.

Surfactants are commonly used to stabilize cells and create foams with a uniform cell size. Method 1 is a simple, one-step process favored for industrial applications. However, the foam prepared using this method demonstrates a relatively large variation in cell size, as illustrated in Figure 8(a). The variation can be reduced by incorporating Tegostab B 8993 surfactant into the formulation. Figure 10(a) presents SEM images of a foam sample produced using Method 1 with the added surfactant. The cells in this foam exhibit a significantly more uniform size. Micro-CT images of three cross sections of the foam further validated this (Figure 10(b)). The porosity of the foam was determined to be 68%. Thus, the inclusion of the surfactant did not result in higher porosity but enhanced the uniformity of the foam.

To prepare a thin foamed layer that is suitable for artificial leather fabrication, the formulation containing the surfactant was precured at 120°C for 60 min, and then applied on a glass panel using a drawdown bar. The coated glass panel was placed in an oven at 160°C for 30 min to complete the curing and foaming processes. A

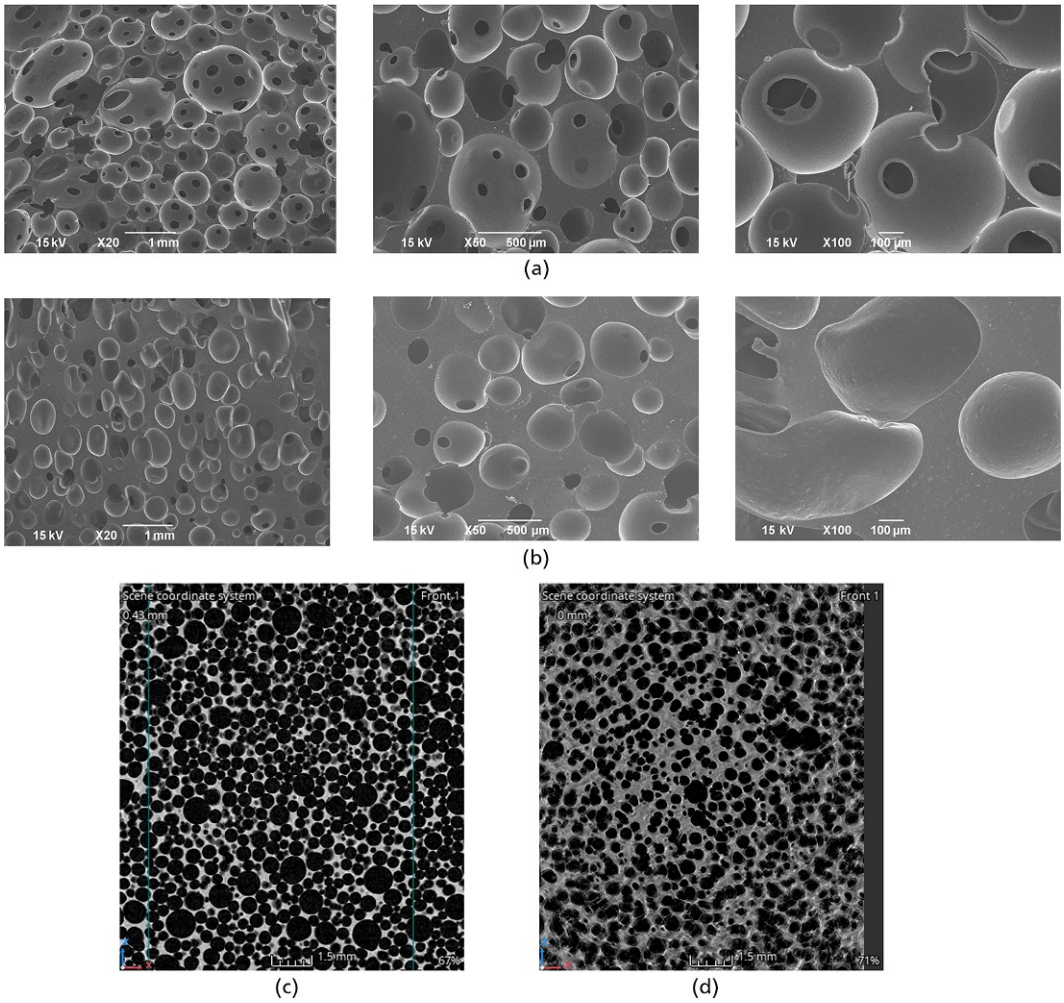

Figure 8. SEM images of foamed samples prepared by Method 1 (a) and Method 2 (b); micro-CT images of foamed samples prepared by Method 1 (c) and Method 2 (d)

Table 4. Foam properties measured by micro-CT

Sample/ preparation method	Total volume: mm^3	Material volume: mm^3	Air volume: mm^3	Material: %	Air: %
Method 1	1722.629	439.903	1282.726	25.53	74.46
Method 2	1833.431	907.554	925.877	49.50	50.50

soft, highly flexible foamed layer was obtained after removing the product from the panel, as shown in Figure 11 and Video 2.

3.3 Fabric layer of bio-based leather

As mentioned earlier, the bottom layer of artificial leather is typically made of fabrics, either woven or nonwoven. Woven textiles are generally more durable and stronger than nonwoven ones and therefore are often preferred in leather fabrication. Since both the top and foamed layers are made of cottonseed oil–based resin in this study, it makes sense to choose cotton fabrics as the bottom layer so that the entire leather structure is derived from cotton. The fabric layer is often adhered to the foamed layer using adhesives in the industry. The formulation for producing the top layer is a natural choice for adhesive because this approach eliminates the need for additional materials for producing cotton-based artificial leather.

3.4 Preparation of leather prototypes

To produce leather prototypes, a piece of 100% warp knit cotton was secured onto a glass substrate using polytetrafluoroethylene-coated fiberglass tape. The formulations for the top and foamed layers were prepared according to procedures detailed earlier in this work. The fabric was then saturated with the top-layer formulation and cured at 160°C for 10 min. This step was necessary to prevent the foamed-layer formulation from being absorbed into the cotton fabric and to ensure strong bonding between the foamed layer and the fabric. The foamed-layer and the top-layer

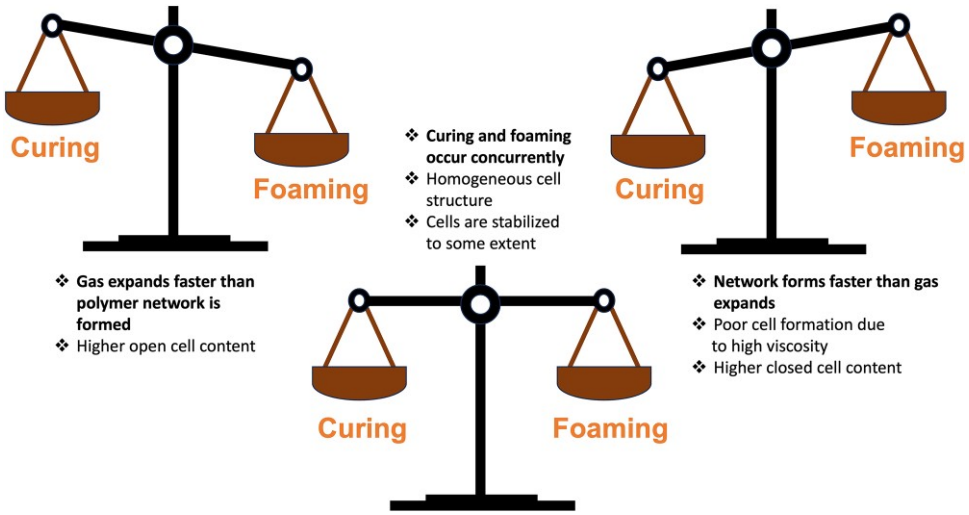

Figure 9. Impact of curing/foaming equilibrium on properties of the foams

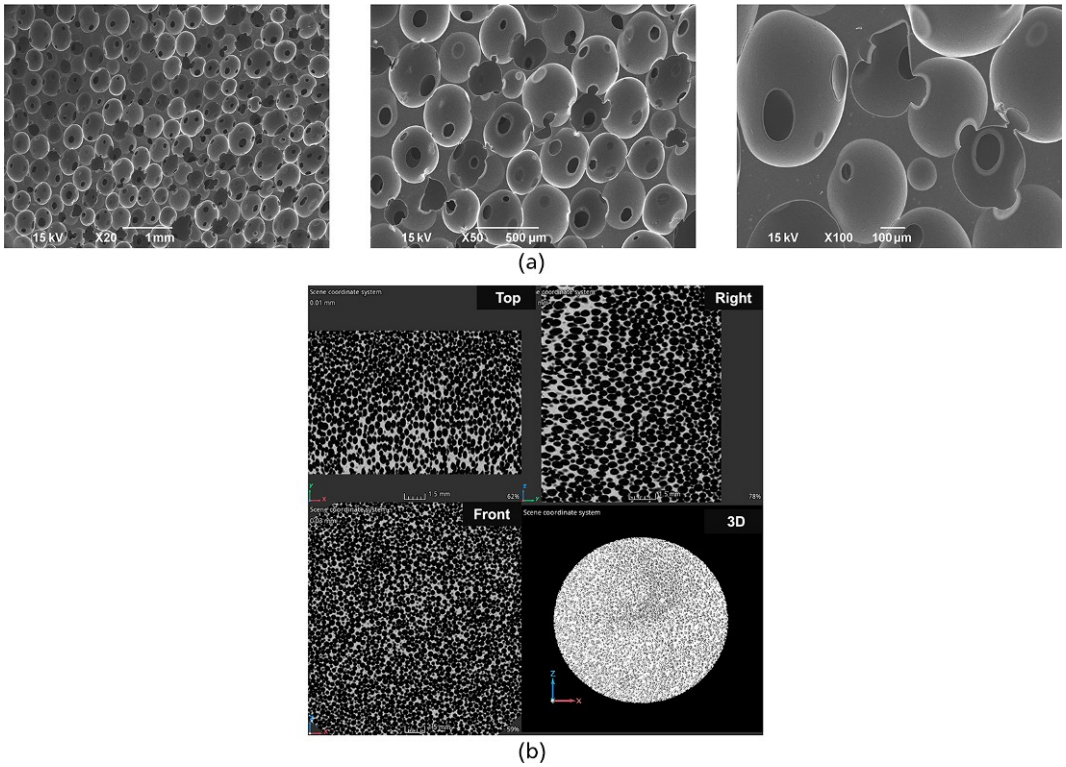

Figure 10. (a) SEM images of the foam sample containing a surfactant in the formulation and (b) micro-CT images of the foam sample containing a surfactant in the formulation

formulations were then applied sequentially to the fabric and placed in the oven at 160°C for 30 min. This batch production method allows for relatively quick production of the leather. The leather prototype made by this batch process is shown in Figure 12 and Video 3.

It should be noted that the leather-like appearance of the leather prototype can be adjusted by using textured rollers, as mentioned earlier. DMA was performed on the leather prototype to evaluate its basic thermomechanical properties and compare them to those of the top layer. The temperature dependence of

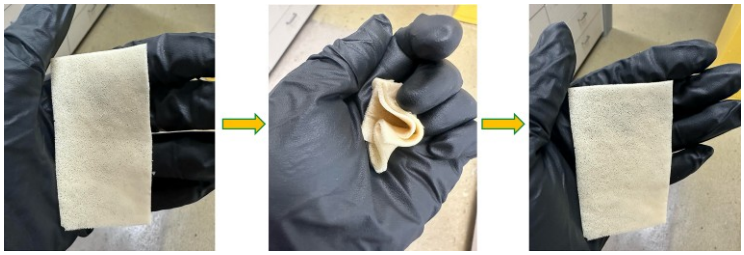

Figure 11. Demonstration of the high flexibility of the foamed layer

Figure 12. ECO-based leather prototype

tan delta and storage modulus of the sample are shown in Figure 13. The glass transition temperature, defined as the tan delta peak temperature, is 32.3°C, whereas the storage modulus in the rubbery plateau region is 9.4 MPa. These values are higher than those of the top layer (Figure 6(b)), which is expected due to the presence of the cotton fabric as a reinforcement to the material. The presence of the porous foamed layer did not diminish the thermomechanical properties of the leather prototype. This is attributed to the thermosetting nature of the foamed layer, which is made from the ECO-based polymer matrix. Overall, the leather prototype exhibits excellent flexibility and good mechanical strength.

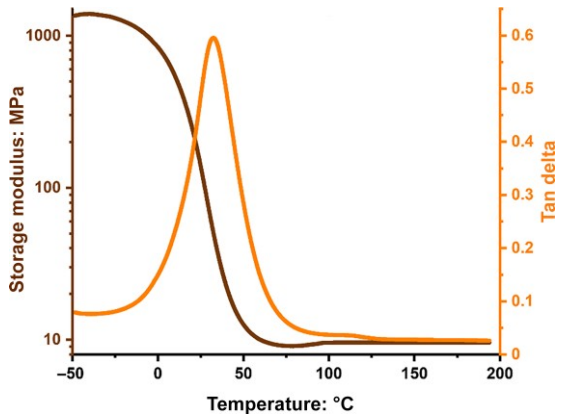

Figure 13. Temperature dependence of tan delta and storage modulus for the leather prototype

The batch process developed in this study for creating ECO-based artificial leather can be adapted to continuous or semi-continuous processes currently employed in the artificial leather industry. Production lines utilizing conveyor ovens can manufacture the new leather without requiring major changes. It is important to note that this study focuses on formulation and parameter development. Systematic property characterization of the leather falls outside the current scope and can be addressed in future research.

4. Conclusions

While most contemporary artificial leather is produced in a more environmentally friendly manner than genuine leather, it still falls short of adhering to the principles of green chemistry. This research seeks to enhance the sustainability of artificial leather by utilizing bio-based materials to create all three layers of typical artificial leather. The top and foamed layers with desirable properties were successfully developed using ECO as the primary ingredient. The formulations and processes applied to produce these two layers were optimized based on thermomechanical properties, chemical resistance, microstructure, and hand feel. The conditions can also be further tailored to meet specific property requirements. Prototype ECO-based artificial leather was created through a layer-by-layer batch process using cotton fabric as the base layer and the top-layer formulation as the adhesive to eliminate the need for other non-bio-based chemicals. Consequently, all three layers of this innovative artificial leather are derived from cotton. This new leather has the potential to serve as a replacement for petrochemical synthetic leathers like those made from PVC and PU.

Author contributions

Marta-Ievheniia Vonsul, Investigation, Visualization, Writing – Original draft. Austin Knight, Investigation. Mohammad Sabzi, Investigation. Renuka Dhandapani, Funding acquisition. Long Jiang, Funding acquisition, Supervision, Writing – Review and editing. Dean C. Webster, Funding acquisition, Supervision, Writing – Review and editing.

Declaration of competing interest

The authors declare no competing interests.

Funding

Funding for this work from Cotton, Incorporated, is gratefully acknowledged.

Acknowledgements

Authors also acknowledge the NDSU Electron Microscopy Center core facility for the SEM analysis and Micro-CT (This material is based upon work supported by the National Science Foundation under Grant Nos. 0619098 and 1229417. Any opinions, findings, and conclusions or recommendations expressed in this material are those of the author(s) and do not necessarily reflect the views of the National Science Foundation).

REFERENCES

1. Ding W, Zhang Y, Li S *et al.* (2023) Novel biomass-based polymeric dyes: preparation and performance assessment in the dyeing of biomass-derived aldehyde-tanned leather. *Polymers* **15**: 2300.
2. Yu Y, Lin Y, Zeng Y *et al.* (2021) Life cycle assessment for chrome tanning, chrome-free metal tanning, and metal-free tanning systems. *ACS Sustainable Chemistry & Engineering* **9**: 6720–6731.
3. Meyer M, Dietrich S, Schulz H and Mondschein A (2021) Comparison of the technical performance of leather, artificial leather, and trendy alternatives. *Coatings* **112**: 226.
4. Kniep J, Graupner N, Reimer JJ and Müssig J (2024) Mycelium-based biomimetic composite structures as a sustainable leather alternative. *Materials Today Communications* **39**: 109100.
5. Kanagaraj J, Panda RC and Kumar V (2020) Trends and advancements in sustainable leather processing: future directions and challenges: a review. *Journal of Environmental Chemical Engineering* **8**: 104379.
6. Saravanabhavan S, Thanikaivelan P, Rao JR, Nair BU and Ramasami T (2006) Reversing the conventional leather processing sequence for cleaner leather production. *Environmental Science & Technology* **403**: 1069–1075.
7. Borlandelli CM and Mahltig B (2022) Leather types and fiber-based leather alternatives-an overview on selected materials, properties, microscopy, electron dispersive spectroscopy EDS and infrared spectroscopy. *Ann Textile Eng Fashion Technol* **11**: 1001.
8. Choi Y-H and Lee K-H (2021) Ethical consumers' awareness of vegan materials: focused on fake fur and fake leather. *Sustainability* **13**: 436.
9. Rathinamoorthy R and Kiruba T (2020) Bacterial cellulose—a sustainable alternative material for footwear and leather products. In *Leather and Footwear Sustainability: Manufacturing, Supply Chain, and Product Level Issues*, pp. 91–121.
10. Yang C, Wang J and Li L (2017) A novel approach for developing high thermal conductive artificial leather by utilizing smart electronic materials. *Textile Research Journal* **877**: 816–828.
11. Defonseka C (2022) *Polymeric Coating Systems for Artificial Leather: Standard and Latest Technologies*. Walter de Gruyter GmbH & Co KG.
12. Narayanan P and Janardhanan SK (2024) An approach towards identification of leather from leather-like polymeric material using FTIR-ATR technique. *Collagen and Leather* **61**: 1.
13. Shahid MA, Miah MS and Razzaq MA (2023) Fabrication of ecofriendly jute fiber reinforced flexible planar composite as a potential alternative of leather. *Journal of Engineered Fibers and Fabrics* **18**: 15589250221144015.
14. Sun Z, Ren S, Wu T *et al.* (2022) A self-matting waterborne polyurethane coating for PVC artificial leather. *Polymers* **151**: 127.
15. Xu M, Cao C, Hu H *et al.* (2022) Perspective on the disposal of PVC artificial leather via pyrolysis: Thermodynamics, kinetics, synergistic effects and reaction mechanism. *Fuel* **32**: 125082.
16. Ma J, Cai K, Yang C *et al.* (2022) Synthesis and properties of photocurable polyurethane acrylate for textile artificial leather. *Progress in Organic Coatings* **171**: 107017.
17. Gurera D and Bhushan B (2018) Fabrication of bioinspired superliquiphobic synthetic leather with self-cleaning and low adhesion. *Colloids and Surfaces A: Physicochemical and Engineering Aspects* **545**: 130–137.
18. Ritter SK (2014) Synthetic leather's green revival. *Chemical & Engineering News* **92**: 28–29.
19. Kinge A, Landage S and Wasif A (2013) Nonwoven for artificial leather. *Int. J. Adv. Res. Eng. Appl. Sci* **218**: 18–33.
20. Roh EK (2020) Mechanical properties and preferences of natural and artificial leathers, and their classification with a focus on leather for bags. *Journal of Engineered Fibers and Fabrics* **15**: 1558925020968825.
21. Xu W and Liu D (2024) High solid content waterborne polyurethane with high foaming rate to artificial leather: Synthesis and characterization. *Progress in Organic Coatings* **18**: 108332.
22. Wjunow C, Moselewski K-L, Huhnen Z, Sultanova S and Sabantina L (2023) Sustainable textiles from unconventional biomaterials—cactus based. *Engineering Proceedings* **37**: 58.
23. Amobonye A, Lalung J, Awasthi MK and Pillai S (2023) Fungal mycelium as leather alternative: a sustainable biogenic material for the fashion industry. *Sustainable Materials and Technologies* **38**: e00724.
24. Patil H, Patil Y, Maiti S, Athalye A and Adivarekar RV (2024) Valorization of fruit vegetable waste for semi-synthetic leather. *Iranian Polymer Journal* **335**: 597–605.
25. Basak S, Shakyawar D, Samanta KK *et al.* (2022) Development of natural fibre based flexural composite: a sustainable mimic of natural leather. *Materials Today Communications* **32**: 103976.
26. Tian Y, Wang J, Zheng S, He X and Liu X (2022) Research on the preparation and application of synthetic leather from coffee grounds for sustainable development. *Sustainability* **14**: 13971.
27. Hijosa CAA (2015) *Piñatex, the Design Development of a New Sustainable Material*. Royal College of Art, United Kingdom.
28. Tewari S, Reshamwala SM, Bhatt L and Kale RD (2024) Vegan leather: a sustainable reality or a marketing gimmick? *Environmental Science and Pollution Research International* **313**: 3361–3375.
29. Pešić M, Nemeša I, Bukhonka N and Bozoki V Fruit based sustainable textile materials. *9th International Joint Conference on Environmental and Light Industry Technologies*. Hungary.
30. Stewart BA, Alegria LA, Totman RJ and Avniel YC (2021) Fungal textile materials and leather analogs. *Google Patents*.
31. Ross P, Wenner N and Moorleghen C (2020) Method of producing fungal materials and objects made therefrom. *Google Patents*.
32. Jones M, Gandia A, John S and Bismarck A (2020) Leather-like material biofabrication using fungi. *Nature Sustainability* **41**: 9–16.

33. Rodrigues I, Mata TM and Martins AA (2022) Environmental analysis of a bio-based coating material for automobile interiors. *Journal of Cleaner Production* **367**: 133011.
34. Mogas-Soldevila L, Matzeu G, Presti ML and Omenetto F (2021) Additively manufactured leather-like silk protein materials. *Materials & Design* **203**: 109631.
35. Williams E, Cenian K, Golsteijn L, Morris B and Scullin ML (2022) Life cycle assessment of MycoWorks' reishi™: the first low-carbon and biodegradable alternative leather. *Environmental Sciences Europe* **34**: 120.
36. Kim JR and Sharma S (2012) The development and comparison of bio-thermoset plastics from epoxidized plant oils. *Industrial Crops and Products* **361**: 485–499, 10.1016/j.indcrop.2011.10.036.
37. Demchuk Z, Shevchuk O, Tarnavchyk I *et al.* (2016) Free radical polymerization behavior of the vinyl monomers from plant oil triglycerides. *ACS Sustainable Chemistry & Engineering* **4**: 6974–6980, 10.1021/acssuschemeng.6b01890.
38. Meshram PD, Puri RG, Patil AL and Gite VV (2013) Synthesis and characterization of modified cottonseed oil based polyesteramide for coating applications. *Progress in Organic Coatings* **76**: 1144–1150.
39. Jian X-Y, An X-P, Li Y-D *et al.* (2017) All plant oil derived epoxy thermosets with excellent comprehensive properties. *Macromolecules* **50**: 5729–5738.
40. Paramarta A and Webster DC (2016) Bio-based high performance epoxy-anhydride thermosets for structural composites: the effect of composition variables. *Reactive and Functional Polymers* **105**: 140–149.
41. Llevot A (2017) Sustainable synthetic approaches for the preparation of plant oil-based thermosets. *Journal of the American Oil Chemists' Society* **94**: 169–186.
42. Lerma-Canto A, Samper MD, Dominguez-Candela I, Garcia-Garcia D and Fombuena V (2023) Epoxidized and maleinized hemp oil to develop fully bio-based epoxy resin based on anhydride hardeners. *Polymers* **15**: 1404.
43. Pan X and Webster DC (2011) Impact of structure and functionality of core polyol in highly functional biobased epoxy resins. *Macromolecular Rapid Communications* **32**17: 1324–1330.
44. Cogliano T, Turco R, Di Serio M *et al.* (2024) Epoxidation of vegetable oils via the prilezhaev reaction method: a review of the transition from batch to continuous processes. *Industrial & Engineering Chemistry Research* **63**: 11231–11262.
45. Nelson TJ, Galhenage TP and Webster DC (2013) Catalyzed crosslinking of highly functional biobased epoxy resins. *Journal of Coatings Technology and Research* **10**: 589–600.
46. Zhang Z, Jiang P, Liu D *et al.* (2021) Research progress of novel bio-based plasticizers and their applications in poly (vinyl chloride). *Journal of Materials Science* **56**: 10155–10182.
47. Carbonell-Verdu A, Samper MD, Garcia-Garcia D, Sanchez-Nacher L and Balart R (2017) Plasticization effect of epoxidized cottonseed oil (ECSO) on poly (lactic acid). *Industrial Crops and Products* **104**: 278–286.
48. Bouti M, Irinislimane R and Belhaneche-Bensemra N (2022) Properties investigation of epoxidized sunflower oil as bioplasticizer for poly (lactic acid). *Journal of Polymers and the Environment* **30**: 232–245.
49. Vonsul M-I and Webster DC (2023) Investigation of cottonseed oil as renewable source for the development of highly functional UV-curable materials. *Progress in Organic Coatings* **185**: 107883.
50. Hill LW (1997) Calculation of crosslink density in short chain networks. *Progress in Organic Coatings* **31**: 235–243.
51. Vonsul M-I, Dhandapani R and Webster DC (2024) Unlocking the potential of functionalized cottonseed oil for the production of biobased epoxy foams. *Industrial Crops and Products* **222**: 119735, 10.1016/j.indcrop.2024.119735.
52. Artavia L and Macosko C (1990) Foam kinetics. *Journal of Cellular Plastics* **26**: 490–511.
53. Ding Y, Qi C, Chen Q *et al.* (2024) Computational modeling and simulation of temperature field evolution during the chemical foaming of epoxy foams. *Polymer Engineering & Science* **64**: 1312–1325.
54. Wypych G (2022) *Handbook of Foaming and Blowing Agents*. Elsevier.